



Free vibration analysis of oil pipes embedded in viscous fluid

Hasan Rahimipour^a

^a Pars Oil and Gas Co, Iran

* Corresponding author e-mail: hasan_pogc@yahoo.com

Abstract

The free vibration of oil pipes embedded in viscous fluid is investigated based on Euler-Bernoulli beam model. The governing equations are developed by Hamilton's principle, including the effects of external viscous fluid, temperature change and length. The effect of the external viscous fluid is simulated as an external force. Applying DQ approach, the resulting equations are transformed into a set of eigenvalue equations. The vibration characteristics of the embedded oil pipes are described and the effects of the design parameters and mode numbers on the frequencies are also examined. Most results presented in the present investigation have been absent from the literature for the vibration of the embedded oil pipes. It is shown that the effect of aspect ratio on frequency is significant for the oil pipes with higher aspect ratio. Finally, it is hoped that the results proposed in this investigation would be helpful for the design of the oil pipes.

Keywords: Free vibration; Oil pipes; Viscous fluid; Euler-Bernoulli beam.

1. Introduction

Pipes conveying fluid have become one of the important structures widely used in engineering, such as those employed in nuclear reactor, ocean mining, heat exchanger, drug delivery, microfluidic and nanofluidic devices [1-6]. In such applications, one of the most important issues is to accurately measure the vibration characteristics, such as natural frequency, stability and critical flow velocity of the fluid-conveying systems. It is not surprising, therefore, that the study on this topic is constantly expanding in the past decades. Indeed, the vibration and stability of pipes conveying fluid have been studied for more than six decades, both theoretically and experimentally. A good review of the related literature was provided by Païdoussis and Li [1]. As for the literature published so far, it is noted that several methods have been used to solve the vibration problem of such structures both in linear and nonlinear dynamics, such as Galerkin method [7-13], DQM [14-16], finite element method (FEM) [17-20], power series expansion and D-decomposition method [21], etc.

In this study, the differential transformation method (DTM) is employed to investigate the free vibration of pipes conveying fluid with different boundary conditions. The DTM was first proposed by Zhou [22] for solving linear and non-linear initial value problems in electrical circuit

analysis. Based on Taylor's series expansion, the DTM provides an effective and simple means of solving linear and non-linear differential equations. By using DTM, Chen and Ho [23] investigated the eigenvalues of Sturm-Liouville problem. They [24] also used this method to study the transverse vibration of rotating twisted Timoshenko beams under axial loading. Mei [25] utilized the DTM to analyze the free vibration of a centrifugally stiffened beam. Muge and Metin [26] adopted the DTM to analyze the vibration of an elastic beam supported on elastic soil. Chen and Chen [27] studied the free vibration of a conservative oscillator with inertia and static cubic non-linearity and pointed out that the DTM has the inherent ability to deal with non-linear problems and it can be employed for the solutions of both ordinary and partial differential equations. In a latest literature, Odibat et al. [28] proposed a reliable new algorithm of DTM, namely multi-step DTM, which will increase the interval of convergence for the series solution, and applied the multi-step DTM to study the non-chaotic and chaotic dynamics of Lotka-Volterra, Chen and Lorenz systems. A generalized differential transform method (GDTM), i.e., the differential transform-Padé technique, mixed by DTM and Padé approximation, was proposed and used to solve differential-difference equation successfully by Zou et al. [29]. Very recently, Chen et al. [30] studied the natural frequencies and mode shapes of marine risers with different boundary conditions by using the DTM.

From a mathematical point of view, in fact, the DTM displays its advantage in many computational problems governed by differential equations. As an example, Chen and Chen [31] investigated the free behavior of a strongly non-linear oscillator with fifth-order non-linearities and showed that the DTM is a powerful tool for solving non-linear problems. They also pointed out that the DTM provides an accurate and efficient way for solving differential equations with high-order non-linearities. Kurnaz et al. [32] generalized the DTM to n-dimensional cases for solving partial differential equations (PDEs) with n-variables. It was shown that the DTM is a feasible tool to solve n-dimensional linear or nonlinear PDEs.

The organization of this paper is as follows. In section 2, the theoretical background of the DTM is reviewed. In section 3, the equation of motion of pipes conveying fluid with several boundary conditions is given, and the differential transformation of the equation of motion is derived. Solution procedure of DTM is also presented in section 3. In section 4, numerical results are given and compared with those obtained by DQM and with other results reported previously, and good agreement is found. Conclusions are given in the last section.

2. Derivation of the motion equations

A oil pipe (of length L), which is described as a Euler-Bernoulli beam embedded in viscous fluid, is considered. Using the Euler-Bernoulli beam theory, the displacement fields are of the form:

$$\begin{aligned}\tilde{U}(x, z, t) &= U(x, t) - z \frac{\partial W(x, t)}{\partial x}, \\ \tilde{V}(x, z, t) &= 0, \\ \tilde{W}(x, z, t) &= W(x, t).\end{aligned}\tag{1}$$

where U and W denote the longitudinal and transverse displacements of the middle surface, respectively. Using Eq. (1), the strain-displacement relation can be written as:

$$\begin{aligned}\varepsilon_{xx}(x, z) &= \frac{\partial \tilde{U}}{\partial x} + \frac{1}{2} \left(\frac{\partial W}{\partial x} \right)^2, \\ \varepsilon_{zz}(x, z) &= 0, \\ \gamma_{xz}(x, z) &= 0,\end{aligned}\tag{2}$$

The total potential energy, V , of oil pipe is the sum of strain energy, U_s , the kinetic energy, K_{tube} , and the external work, W_v , which is expressed as:

$$V = K_{tube} - (U_s - W_v), \quad (3)$$

where, total electrostatic energy can be expressed as:

$$U_s = \frac{1}{2} \int_0^L \int_A (\sigma_{xx} \varepsilon_{xx}) dA_i dx, \quad (4)$$

Using the resultant forces and moments in the middle surface of pipe which are defined as:

$$N_x = \int_A \sigma_x dA, \quad (5)$$

$$M_{xi} = \int_A \sigma_{xx} z dA, \quad (6)$$

the total strain energy can be written as:

$$U_s = \frac{1}{2} \int_0^L \left[N_x \frac{\partial U}{\partial x} + \frac{1}{2} N_x \left(\frac{\partial W}{\partial x} \right)^2 - M_x \frac{\partial^2 W}{\partial x^2} \right] dx \quad (7)$$

The kinetic energy of pipe is given by:

$$K = \frac{1}{2} \rho_t \int_0^L \left[\int_{A_1} \left[\left(\frac{\partial \tilde{U}_1}{\partial t} \right)^2 + \left(\frac{\partial \tilde{W}_1}{\partial t} \right)^2 \right] dA_1 + \int_{A_2} \left[\left(\frac{\partial \tilde{U}_2}{\partial t} \right)^2 + \left(\frac{\partial \tilde{W}_2}{\partial t} \right)^2 \right] dA_2 \right] dx. \quad (8)$$

kinetic energy of flow fluid is given as follow:

$$K_{fluid} = \frac{1}{2} \rho_f \int_0^L \int_{A_f} \left\{ \left(\frac{\partial \tilde{U}_1}{\partial t} + U_f \cos \theta \right)^2 + \left(\frac{\partial \tilde{W}_1}{\partial t} - U_f \sin \theta \right)^2 \right\} dA_f dx, \quad (9)$$

and fluid external work due to centripetal force is:

$$W_{vfluid} = - \int_0^L \int_{A_f} \left\{ m_f U_f^2 \frac{\partial^2 W_1}{\partial x^2} \cos \theta W_1 + m_f U_f^2 \frac{\partial^2 W_1}{\partial x^2} \sin \theta U_1 \right\} dA_f dx. \quad (10)$$

To evaluate the viscosity effect for oil pipe, Navier-stokes equation can be used as as:

$$\rho_f \frac{d\vec{V}}{dt} = -\nabla P + \mu \nabla^2 \vec{V}. \quad (11)$$

Substituting the fluid velocity in Eq. (11) yields:

$$\left[\frac{\partial}{\partial t} + U_f \frac{\partial}{\partial x} \right] \left[\frac{\partial \tilde{U}_1}{\partial t} + U_f \cos \theta \right] = -\frac{\partial P}{\partial x} + \mu \frac{\partial^2}{\partial x^2} \left[\frac{\partial \tilde{U}_1}{\partial t} + U_f \cos \theta \right], \quad (12)$$

$$\left[\frac{\partial}{\partial t} + U_f \frac{\partial}{\partial x} \right] \left[\frac{\partial W_1}{\partial t} - U_f \sin \theta \right] = -\frac{\partial P}{\partial z} + \mu \frac{\partial^2}{\partial x^2} \left[\frac{\partial W_1}{\partial t} - U_f \sin \theta \right]. \quad (13)$$

It should be noted that applying surface integrals ($m = \int_A \rho dA$) to above equations, viscosity terms were derived and added to equation of motion. The external work due to surrounding viscous fluid is:

$$W_v = \int_0^L q W dx. \quad (14)$$

The surface traction of the external fluid along the interface can be given by

$$q = -\alpha \frac{\partial W}{\partial t}, \quad (15)$$

where

$$\alpha = \frac{2\nu_f \pi (\eta^2 - 1)}{(1 - \eta^2 + (\eta^2 + 1) \ln \eta)}, \quad \eta = \frac{R_o}{R_i} \quad (16)$$

It should be noted that the parameter α is positive ($0 < \alpha < 1$). Here, R_o is pipe outer radius and R_i is the distance from the center line to the position where the induced viscous flow vanished. To couple the elastic deformation of the pipe and the viscous flow of the external fluid, we assume that the surface traction of the external fluid along the interface is equal to external force exerted on the pipe.

The motion equations of embedded oil pipe conveying viscose fluid can be derived by Hamilton's principles as follows:

$$\int_0^t \delta (K - (U_s - W_v)) dt = 0. \quad (17)$$

Integrating Eq. (17) by parts and setting the coefficient of mechanical and electrical to zero lead to the following motion equations:

$$\frac{\partial N_x}{\partial x} = \rho h \frac{\partial^2 U}{\partial t^2}, \quad (18)$$

$$\frac{\partial^2 M_x}{\partial x^2} - \frac{\partial}{\partial x} \left(N_M \frac{\partial W}{\partial x} \right) + q = \rho h \frac{\partial^2 W}{\partial t^2} - \rho_t I_1 \frac{\partial^4 W}{\partial x^2 \partial t^2}, \quad (19)$$

3. Solution method

In this section, the differential quadrature method (DQM) is used to solve the motion equations. In this method the partial derivative of a function with respect to spatial variables at a given discrete point are approximated as a weighted linear sum of the function values at all discrete points

chosen in the solution domain. According to this method, the functions u_i, w_i and their derivatives are approximated as:

$$\frac{\partial^k}{\partial \zeta^k} \{u_i, w_i, \phi_i\} \Big|_{\zeta=\zeta_j} = \sum_{m=1}^N C_{jm}^{(k)}(\zeta) \{u_{im}(\zeta_m, t), w_{im}(\zeta_m, t), \phi_{im}(\zeta_m)\}, \quad i=1,2 \quad (20)$$

where N is the grid points along ζ and $C_{jm}^{(k)}$ represent the Lagrange interpolation polynomial and its k th derivative, that can be found in [1]. The solution of the motion equations can be assumed as follows:

$$u_i(x, t) = u_i(x) e^{i\omega t}, \quad (21)$$

$$w_i(x, t) = w_i(x) e^{i\omega t}, \quad (22)$$

Imposing the above boundary conditions into Eqs. (18) to (19) leads to the following constitutive matrix equation as:

$$([K] + \Omega[C] + \Omega^2[M]) \begin{pmatrix} d_b \\ d_d \end{pmatrix} = 0, \quad (23)$$

where the subscript b stands for the elements related to the boundary points while subscript d is associated with the remainder elements. The $[K]$, $[C]$ and $[M]$ are the stiffness matrix, damping matrix and mass matrix, respectively. For solving the Eq. (23) and reducing it to the standard form of eigenvalue problem, it is convenient to rewrite Eq. (23) as the following first order variable as:

$$\{\dot{Z}\} = [A]\{Z\}, \quad (24)$$

in which the state vector Z and state matrix $[A]$ are defined as:

$$Z = \begin{Bmatrix} d_b \\ \dot{d}_b \end{Bmatrix} \quad \text{and} \quad [A] = \begin{bmatrix} [0] & [I] \\ -[M^{-1}K] & -[M^{-1}C] \end{bmatrix}, \quad (25)$$

where $[0]$ and $[I]$ are the zero and unitary matrices, respectively. However, the frequencies obtained from the solution of Eq. (24) are complex due to the damping existed in the presence of the viscous fluid flow. Hence, the results are containing two real and imaginary parts. The real part is corresponding to the system damping, and the imaginary part representing the system natural frequencies.

4. Numerical results

In the following subsections, based on the numerical method mentioned in section 3, the nonlinear frequency and critical fluid velocity of the oil pipe are obtained so that the effects of aspect ratio, fluid viscosity and fluid velocity of fluid on the natural frequency and instability of the oil pipes are studied and discussed in details.

Fig. 1 shows the geometrical aspect ratio (η) on the natural frequency of oil pipe versus flow velocity. As can be seen, natural frequency decreases with increasing flow velocity. These imply that the system is stable. When the natural frequency becomes zero, critical velocity is reached, which the system loses its stability due to the divergence via a pitchfork bifurcation. In this state, both real and imaginary parts of frequency become zero at the same point. Therefore, with

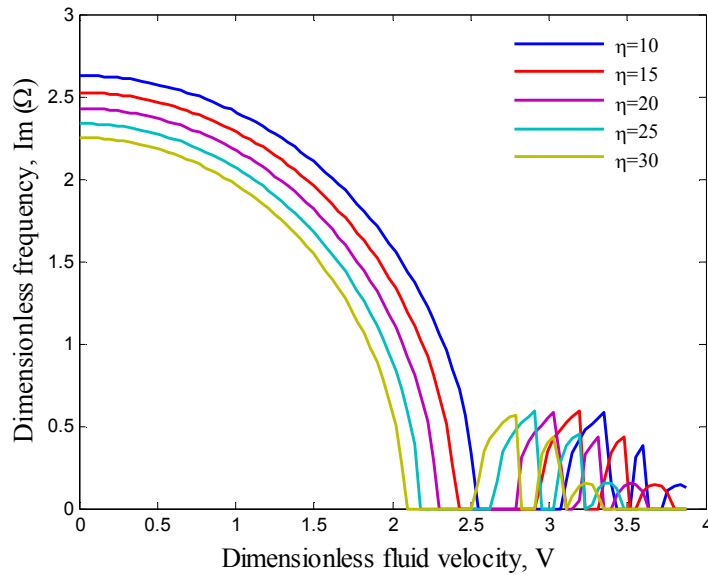


Figure 1. Natural frequency versus fluid velocity for different aspect ratio.

increasing flow velocity, system stability decreases and became susceptible to buckling. It can be observed that the oil pipe becomes unstable at $u_f = 2.52$ for the $\eta = 10$ while it reduces significantly with increasing geometrical aspect ratio. This is because increasing the geometrical aspect ratio implies decreasing interaction force between pipe atoms, and that leads to a softer structure.

Figs. 2 illustrates the effect of fluid viscosity on the natural frequency of oil pipe versus flow velocity. The results indicating that viscous fluid increases natural frequency. However, during the flow of a fluid through a pipe, modelled as a Euler-Bernoulli beam, the effect of fluid viscosity on the vibration and instability of oil pipe may be ignored at lower fluid velocity.

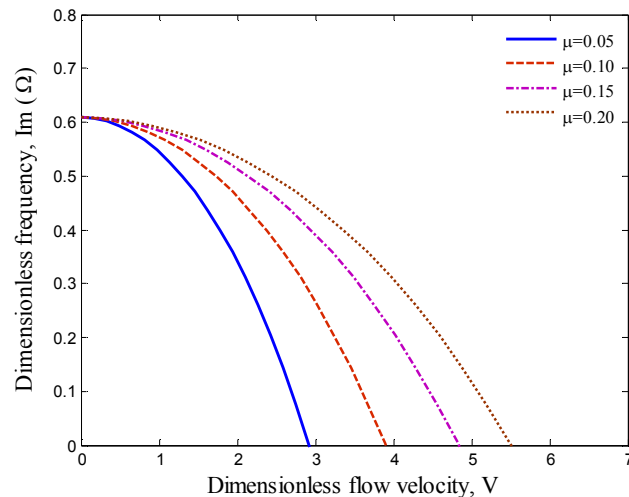


Figure 2. Natural frequency versus fluid velocity for different fluid viscosity.

5. Conclusion

In the present study, free vibration of oil pipes embedded in viscous fluid is investigated based on Euler-Bernoulli beam model. Using energy method and Hamilton's principle, the motion

equations are derived. The effect of the external viscous fluid is simulated as an external force. Furthermore, the effect of internal fluid is simulated using Navier-stokes equation. Applying DQ approach, the resulting equations are transformed into a set of eigenvalue equations. The vibration characteristics of the embedded oil pipes are described and the effects of the design parameters on the frequencies are also examined. Most results presented in the present investigation have been absent from the literature for the vibration of the embedded oil pipes. It is shown that the effect of aspect ratio on frequency is significant for the oil pipes with higher aspect ratio. Finally, it is hoped that the results proposed in this investigation would be helpful for the design of the oil pipe.

References

1. Païdoussis MP, Li GX. Pipes conveying fluid: a model dynamical problem. *J Fluids Struct* 1993;7:137-204.
2. Rinaldi S, Prabhakar S, Vengallator S, Païdoussis MP. Dynamics of microscale pipes containing internal fluid flow: Damping, frequency shift, and stability. *J Sound Vib* 2010; 329: 1081-1088.
3. Whitby M, Quirke N. Fluid flow in carbon nanotubes and nanopipes. *Nat Nanotechnol* 2007; 2: 87-94.
4. Wang L. Vibration and instability analysis of tubular nano- and micro-beams conveying fluid using nonlocal elastic theory. *Physica E* 2009; 41: 1835-1840.
5. Wang L. Size-dependent vibration characteristics of microtubes conveying fluid. *J Fluids Struct* 2010; 26: 675-684.
6. Païdoussis MP. *Fluid-Structure Interactions: Slender Structures and Axial Flow*, vol. 1. London, Academic Press;1998.
7. Païdoussis MP, Issid NT. Dynamic stability of pipes conveying fluid. *J Sound Vib* 1974;33: 267-294.
8. Païdoussis MP. Flow-induced instabilities of cylindrical structures. *Appl Mech Rev* 1987;40:163-175.
9. Païdoussis MP, Semler C. Nonlinear and Chaotic Oscillations of a Constrained Cantilevered Pipe Conveying Fluid: A Full Nonlinear Analysis. *Nonlinear Dyn* 1993;4: 655-670.
10. Sarkar A, Païdoussis MP. A cantilever conveying fluid: coherent modes versus beam modes. *Int J Non-Linear Mech* 2004; 39:467-481.
11. Païdoussis MP, Sarkar A, Semler C. A horizontal fluid-conveying cantilever: spatial coherent structures, beam modes and jumps in stability diagram. *J Sound Vib* 2005;280:141-157.
12. Jin JD, Song ZY. Parametric resonances of supported pipes conveying pulsating fluid. *J Fluids Struct* 2005;20:763-783.
13. Wang L. A further study on the non-linear dynamics of simply supported pipes conveying pulsating fluid. *Int J Non-Linear Mech* 2009;44:115-121.
14. Qian Q, Wang L, Ni Q. Instability of simply supported pipes conveying fluid under thermal loads. *Mech Res Commun* 2009; 36(3): 413-417.
15. Wang L, Ni Q. In-plane vibration analyses of curved pipes conveying fluid using the generalized differential quadrature rule. *Comput Struct* 2008; 86(1-2): 133-139.
16. Ni Q, Wang L, Qian Q. Bifurcations and chaotic motions of a curved pipe conveying fluid with nonlinear constraints. *Comput Struct* 2006;84:708-717.
17. Pramila A. On the gyroscopic terms appearing when the vibration of fluid conveying pipe is analyzed using the FEM. *J Sound Vib* 1986; 105: 515-516.

18. Zhang YL, Gorman DG, Reese JM. A finite element method for modelling the vibration of initially tensioned thin-walled orthotropic cylindrical tubes conveying fluid. *J Sound Vib* 2001; 245:93-112.
19. Pramila A, Laukkanen J, Liukkonen S. Dynamics and stability of short fluid-conveying Timoshenko element pipes. *J Sound Vib* 1991; 144:421-425.
20. Olson LG, Jamison D. Application of a general purpose finite element method to elastic pipes conveying fluid. *J Fluids Struct* 1997;11:207-222.
21. Kuiper GL, Metrikine AV. Dynamic stability of a submerged, free-hanging riser conveying fluid. *J Sound Vib* 2005;280:1051-1065.
22. Zhou JK. *Differential transformation and its applications for electrical circuits*. Wuhan, China: Huazhong University Press;1986.
23. Chen CK, Ho SH. Application of differential transformation to eigenvalue problems, *Appl Math Comput* 1996;79:173-188.
24. Chen CK, Ho SH. Transverse vibration of a rotating twisted Timoshenko beams under axial loading using differential transform. *Int J Mech Sci* 1999;41:1339-1356.
25. Mei C. Application of differential transformation technique to free vibration analysis of a centrifugally stiffened beam. *Comput Struct* 2008;86:1280-1284.
26. Balkaya M, Kaya MO, Saglamer A. Analysis of the vibration of an elastic beam supported on elastic soil using the differential transform method. *Arch Appl Mech* 2009;79:135-146.
27. Chen CK, Chen SS. Application of the differential transformation method to a non-linear conservative system. *Appl Math Comput* 2004;154:431-441.
28. Odibat ZM, Bertelle C, Aziz-Alaoui MA, Duchamp GHE. A multi-step differential transform method and application to non-chaotic or chaotic systems. *Comput Math Appl* 2010;59:1462-1472.
29. Zou L, Wang Z, Zong Z. Generalized differential transform method to differential-difference equation. *Phys Lett A* 2009; 373:4142-4151.
30. Chen YF, Chai YH, Li X, Zhou J. An extraction of the natural frequencies and mode shapes of marine risers by the method of differential transformation. *Comput Struct* 2009;87:1384-1393.
31. Chen SS, Chen CK. Application of the differential transformation method to the free vibrations of strongly non-linear oscillators. *Nonlinear Anal RWA* 2009; 10:881-888.
32. Kurnaz A, Oturanç G, Kiris ME. n-Dimensional differential transformation method for solving PDEs. *Int J of Comput Math* 2005; 82: 369-380.